Research Square

Preprints are preliminary reports that have not undergone peer review.
They should not be considered conclusive, used to inform clinical practice,
or referenced by the media as validated information.

Pattern of white matter degeneration in remote brain areas from the basal ganglion lesion of ischemic stroke patients with motor impairment

xuejin cao
Southeast University https://orcid.org/0000-0002-3684-8092
Zan Wang
Southeast University
Xiaohui Chen
Southeast University Zhongda Hospital
Yanli Liu
Southeast University Zhongda Hospital
Xi Yang
Southeast University Zhongda Hospital
Wei Wang
Southeast University Zhongda Hospital
Idriss Ali Abdoulaye
Southeast University
Shiyao Zhang
Southeast University
Xiaoying Guo
Southeast University
Shanshan Wu
Southeast University
Yijing Guo (guoyijingseu@126.com)
https://orcid.org/0000-0002-6638-8963

Research article

Keywords: Ischemic stroke, Diffusion tensor imaging, Structural network, Multivariate pattern analysis , Network-based statistic

Posted Date: July 1st, 2020

DOI: https://doi.org/10.21203/rs.3.rs-36124/v1

License: This work is licensed under a Creative Commons Attribution 4.0 International License.
Read Full License

Abstract

Background

Diffusion tensor imaging (DTI) studies have revealed distinct white matter characteristic of brain following diseases. Beyond the lesion-symptom mapping, recent studies have demonstrate extensive structural and functional alterations of remote areas to local lesions caused by stroke in the brain. Here, we investigated the influences further from a global level by multivariate pattern analysis (MVPA) and network-based statistic (NBS).

Methods

Ten ischemic stroke patients with basal ganglia lesion and motor dysfunction and eleven demographically matched adults underwent brain Magnetic Resonance Imaging scans. DTI data was processed to obtain fractional anisotropy (FA) map and MVPA was used to explore brain regions that play an important role in classification based on FA map. White matter (WM) structural network was constructed by the deterministic fiber tracking approach according to the Automated Anatomical Labeling (AAL) atlas. NBS was used to explore differences of structural network between groups.

Results

MVPA applied to FA images correctly identified stroke patients with a statistically significant accuracy of 100% ($P \leq 0.001$). Compared with the controls, the patients showed an FA reduction in the perilesional basal ganglia and brainstem, with a few in bilateral frontal lobes. Using NBS, we found the significant decreased FA-weighted WM subnetwork in stroke patients.

Conclusions

We identified some patterns of WM degeneration in the affected brain areas remote from the ischemic lesion, revealed the abnormal topological organization of WM network in stroke patients, which may be helpful for understanding of the neural mechanism of stroke sequela.

Background

Local lesions caused by stroke may result in extensive topological alterations of network in the brain. In the past decades, numerous neuroimaging studies have investigated structural and functional reorganization after stroke [1]. Diffusion tensor imaging (DTI) is commonly used to detect structural integrity of the white matter. Previous DTI researches in stroke patients calculated diffusion tensor indicators (e.g. fractional anisotropy (FA), mean diffusivity (MD), radial diffusivity (RD)) in several regions along corticospinal tract (CST) of the lesioned hemisphere and contralateral hemisphere [2, 3], or

computed the integrity of CST [4, 5]. Then these imaging indicators were correlated to function outcome as prediction markers. It has been found certain correlations between the changes of specific fiber bundles and functional outcomes, such as aphasia [6], neglect [7], paralysis [8] and etc. Besides of the command of motor function by CST, other brain areas involving movement control are still fuzzy. Neural degeneration may cause specific functional manifestations, so we made a pattern recognition classification of FA map of the brain in an attempt to explore regions that are closely related with motor function.

Multivariate pattern analysis (MVPA) is a method for analyzing imaging data based on machine learning and pattern recognition. It involves the use of pattern classification algorithms to extract spatial patterns from neuroimaging data, and then sorts individual characteristics [9]. MVPA has the advantage of considering interregional correlations and searching for abnormalities throughout the entire brain, cause it adopts an unbiased and whole-brain method without the region of interest (ROI) be artificially set [10]. This method has been widely used in psychiatric related studies to analyze less severe changes that can be observed in subclinical populations [11, 12].

White matter structural connectivity can be modeled as a network. Network-based statistics (NBS) is a method to control the family-wise error rate when mass univariate testing is performed at every connection comprising the network. So NBS is also a method that investigate of interregional correlations of brain on a global level [13, 14]. For further understanding of the intrinsic brain structural basis of stroke patients with residual motor dysfunction, we used these methods to explore relevant subtle changes and the abnormalities of brain structural networks in ischemic stroke patients.

Methods

Participants

Ten right-handed stroke patients (mean age 56.7 ± 10.5 years) from the Southeast University affiliated Zhongda Hospital between March 2019 and December 2019 were recruited for this study. Inclusion criteria were for patients were as follow:(1) age ≥ 20 and age ≤ 80 years;(2) first-onset ischemic stroke with involvement of the basal ganglia; (3) show pure motor deficits. Exclusion factors: (1) history of neurological or psychiatric disorders; (2) brain abnormalities unrelated to the infarct lesions; (3) MRI contraindications. All of the affected extremities were evaluated for motor function. Motor outcome of limbs on the affected side was evaluated by the Fugl-Meyer assessment (FMA), including for the upper and lower extremity [15]. Also, The Brunnstrom stage (BRS) was adopted. Recovery of the affected extremities was scored on a 6-point scale (1 = severe; 6 = normal) [16]. The clinical characteristics of the stroke patients are summarized in Table 1. Eleven demographically matched healthy controls (mean age 61.5 ± 7.8 years) were recruited.

Table 1
Patient characteristics.

ID	Age (years)	Gender	Side	Localization of infarct	BRS	FMA	Scan time (week)
1	49	F	R	BG	3,3□5	58	22
2	67	F	R	BG	2,1□4	37	2
3	57	F	L	BG□PV	2,1□4	35	4
4	51	M	L	BG□PV	3,2□4	41	10
5	60	M	R	BG□CR	4,4□5	86	20
6	57	M	L	BG□CR	2,1□5	38	3
7	74	M	L	BG□CR□PV	5,4□5	82	14
8	60	M	L	BG	2,1□3	19	2
9	35	M	L	BG	2,1□3	25	3
10	57	M	L	BG	5,5□5	89	24

M = male; F = female; Side: the hemisphere of lesions on brain; IC = internal capsule; CR = corona radiate; BG = basal ganglia; PV = periventricular ; BRS (Brunnstrom stage) : separate functional evaluation of proximal and distal portions of the upper and entire lower extremities. FMA: Fugl-Meyer assessment (full score = 100). Scan time : intervel of DTI acquirement from stroke onset.

Image Acquisition

Diffusion Tensor Images were acquired using a 3.0-Tesla Philips (Ingenia) Medical Systems equipped with a Synergy-L Sensitivity Encoding (SENSE) head coil, using a single echo planar imaging (EPI) sequence, 33 diffusion-weighted images (b = 1000s/mm^2) and a reference T2-weighted image with no diffusion weighting (b = 0 s/mm^2) were obtained with the following acquisition parameters: voxel size = 2 × 2 × 2 mm^3, gap = 0 mm;echo time (TE) = 107 ms; repetition time (TR) = 5835 ms; field of view (FOV) = 256 × 256 mm^2 ; flip angle (FA) = 90°; matrix = 128 × 128; slices = 75 .

High-resolution T1-weighted axial images covering the whole brain were obtained by a 3D-magnetization prepared rapid gradient-echo (MP-RAGE) sequence: TR = 9.6 ms;TE = 3.7 ms; FA = 9°; matrix = 256 × 256; FOV = 256 × 256 mm^2; voxel size = 1 × 1 × 1 mm^3; gap = 0 mm, number of slices = 140. Additionally, sagittal fluid attenuated inversion recovery (FLAIR) images were obtained with the following parameters: TE = 110 ms, TR = 7000 ms, Inversion time (TI) = 2200 ms, FA = 90°, matrix size = 480 × 480, FOV = 250 × 250 mm^2, slice thickness = 5 mm, slices = 20.

Lesion mapping

Lesions of the 7 stroke patients were mainly located in the basal ganglia region in the left hemisphere. For the 3 patients with lesions in the right hemisphere, all the images were laterally flipped to unify the damage side. According to previous investigators, lesion mask for each patient was manually segmented on individual structural MRI images (T1-weighted MP-RAGE and FLAIR images) using MRIcron software (http://www.mricro.com). After the spatial normalization of all individual lesion masks, a lesion overlap image for all patients was constructed (Fig. 1) [17, 18, 19].

DTI Data Pre-Processing and Network Definition

DTI data analysis was performed by a pipeline toolbox for analyzing brain diffusion images (PANDA, http://www.nitrc.org/projects/panda) [20].The main procedure includes: (1) correcting for the head motion and eddy current effect s using the FMRIB's Diffusion Toolbox (FDT); (2) calculating diffusion tensor (DT) metric——FA for each voxel using the DTIFIT tool. (3) normalizing: registrations of all the individual FA images to the FMRIB58_FA template by calling the FNIRT tool [21]. Whole-brain tractography was performed for each subject in the native diffusion space based on fiber assignment by continuous tracking (FACT) algorithm [22]. All voxels with fractional anisotropy (FA) ≥ 0.2 were used as seed points; the FA and curvature thresholds of path tracing were set to 0.2 and 45°, respectively.

An FA weighted network was constructed from 116 nodes defined according to the Automated Anatomical Labeling (AAL) atlas [23]. The entire cerebral cortex was automatically partitioned into 116 anatomical regions of interest (ROIs) (45 ROIs for each cerebral hemisphere, 26 ROIs for cerebellum) using AAL algorithm. The weight of the edges in network were defined as the mean FA value of the connected fibers between each pair nodes. In order to reduce false-positive connections, two nodes were considered structurally connected only when at least 3 fibers were reconstructed between them [24].

Multivariate pattern analysis

Differences in FA values of white matter between groups were examined using a multivariate pattern classification technique. Pattern classification analysis using FA map was implemented in the Pattern Recognition for Neuroimaging toolbox (PRoNTo) (http://www.mlnl.cs. ucl.ac.uk/pronto/) [25]. The area under the receiver operating characteristic curve (AUC) values, sensitivity and specificity of the FA classifications and the weight of each brain region in the classification analysis were obtained.

Statistical Analysis

With respect to inter-nodal connection comparisons, the two-sample t-test are adopted, followed by network-based statistic (NBS) methods using GRETNA (v2.0.0) to analyze FA network between groups. Visualization of the results was performed by the BrainNet Viewer [26, 27].

Two-sample t tests were performed on the two sets of FA maps in SPM12 (false discovery rate (FDR)-corrected $P < 0.05$, cluster size > 5) [28].

Results

Demographic data and Patient characteristics

The mean interval from stroke onset to DTI scans was 10.3 ± 9.0 weeks (Table 1). Stroke lesions were projected to the left hemisphere for each patient and overlaid onto a T1 template in MNI standard space (Fig. 1).

Overall Classifier Performance

Figure 2A shows the result of the MVPA classification between the 10 stroke patients and 11 controls based on FA values. The overall accuracy was 100%, and was significant at $P \leq 0.001$ ($P = 0.001$). The sensitivity was 100%, and the specificity was 100%. The AUC for FA was 1.00 (Fig. 2B).This overall classification accuracy of the algorithm measures its ability to correctly classify the two groups.

Discrimination Map

In the whole-brain voxel weight maps, the weight vector value indicates the relative importance of the voxel in the decision function----- discrimination between patients and controls (Fig. 3). Note that all voxels in the white matter mask contribute to the decision function, since the analysis is multivariate. The spatial distribution of the weight vector provided information about the contribution of different areas to classification.

The brain regions that contributed the most to the discrimination between stroke patients and controls were identified by setting the threshold to ≥ 30% of the maximum weight vector scores, consistent with previous studies using MVPA for disease classification [11, 29]. The most identified classified features of the FA map included the perilesional basal ganglia and brainstem, with a few in bilateral frontal lobes (Figs. 3 and 4).

By comparing the whole-brain FA value of two groups in the discrimination map by SPM12 ($P_{FDR} < 0.05$, cluster size > 5) ,we found stroke group showed reduced FA in left pons, left basal ganglion and a fraction of voxels in bilateral parietal lobe, shown in Fig. 4 and reported in Table 2.

Table 2
Report of FA decreased brain area in patients compared with controls.

ID	Voxels	Peak MNI coordinate(x,y,z)	Peak intensity	Brain regions	
1	36	-4 -36 -46	0.028	Left Brainstem	Pons; Medulla
2	114	-10 -20 -22	0.032	Left Brainstem	Midbrain; Pons
3	112	-22 -6 16	0.027	Left Cerebrum	Extra-Nuclear; Lentiform Nucleus
4	9	-14 -20 60	0.019	Left Cerebrum	Medial Frontal Gyrus
5	7	24 -18 66	0.023	Right Cerebrum	Medial Frontal Gyrus

*ID : the clusters ; Voxels: means the cluster size ; Peak MNI coordinate: indicate the location of voxel with maximum weight vector scores (also peak intensity) in each cluster.

Decreased Connection of the Component Network in stroke patients

FA weighted networks was constructed from the nodes (brain areas) defined according to the AAL atlas. The weight of the edges in network were defined as the mean FA value of the connected fibers between each pair nodes. Network-based statistic (NBS) approach was used on the structural networks constructed by deterministic tractography. We identified significantly decreased connections of a component network (subnetwork) in stroke patients ($P < 0.01$, $P = 0.008$) including 26 regions and 32 connections (Table 3 and Fig. 5A).

Table 3
The 26 brain regions of the subnetwork nodes.

ID	Region	Abbreviation	Side	MNI coordinate		
				x	y	z
1	Precentral	PreCG	L	-39	-6	50.9
2	Dorsolateral Frontal Superior gyrus	SFGdor	L	-18	35	42.2
3	Orbital Frontal Superior	ORBsup	L	-17	47	-13.3
4	Frontal Middle gyrus	MFG	L	-33	33	35.5
5	Orbital Frontal Middle	ORBmid	L	-31	50	-9.6
6	Opercular Frontal Inferior	IFGoperc	L	-48	13	19
7	Supplementary Motor Area	SMA	L	-5	5	61.4
8	Supplementary Motor Area	SMA	R	9	0	61.9
9	Frontal Superior Medial	SFGmed	L	-5	49	30.9
10	Cuneus	CUN	L	-6	-80	27.2
11	Occipital Superior gyrus	SOG	L	-17	-84	28.2
12	Occipital Middle gyrus	MOG	L	-32	-81	16.1
13	Occipital Inferior gyrus	IOG	L	-36	-78	-7.8
14	Postcentral	PoCG	L	-42	-23	48.9
15	Parietal Superior gyrus	SPG	L	-23	-60	59
16	Parietal Inferior gyrus	IPL	L	-43	-46	46.7
17	Precuneus	PCUN	L	-7	-56	48
18	Paracentral Lobule	PCL	L	-8	-25	70.1
19	Caudate	CAU	R	15	12	9.4
20	Putamen	PUT	L	-24	4	2.4
21	Pallidum	PAL	L	-18	0	0.2
22	Thalamus	THA	L	-11	-18	8
23	Cerebellum Crus2	CRBLCrus2	L	-29	-73	-38.2
24	Cerebellum 3	CRBL3	L	-9	-37	-18.6
25	Cerebellum 4_5	CRBL45	L	-15	-43	-16.9
26	Cerebellum 9	CRBL9	L	-11	-49	-45.9

Figure 5 showed the network model that reveal topological changes in brain structural networks in stroke patients. Table 3 reported the regions as nodes in the subnetwork. The backbone matrix of group structural matrixes for each group of the subnetwork was calculated, including the 26 regions in Table 3 (Fig. 5B and C). The subnetwork was composed by cerebral cortical regions (the frontal lobe,the parietal lobe, the occipital lobe), subcortical areas (basal ganglion, thalamus) and part of cerebellum. Compared with the results of MVPA, the changes of frontal parietal lobe and basal ganglia were involved, and the brainstem region may overlap with some of the fibers connected to the cerebellum.

Discussion

Beyond the well-known concept of lesion-symptom mapping, some lesion in a single location in the brain would disrupt brain functions routed to widespread neural networks [1,30]. Our analysis conformed that local destruction of certain anatomic regions can affect remote areas in brain.

White matter degeneration in CST pathway of stroke patients

The degree of anisotropy depends on the level of organization and the integrity of the white matter tract, and on the degree of freedom of water diffusion movement caused by the oriented axonal membranes and myelin sheaths [31]. Reduced anisotropy along the corticospinal tract (CST) remote from a cerebral infarct has been interpreted as Wallerian degeneration (WD) [32]. DTI can quantify the fractional anisotropy (FA) values to evaluate the pathology change of the cerebral white matter, such as WD. By the good classification ability of MVPA, we reported that apart from the basal ganglia region with direct infarcts, brain areas with significantly decreased FA value in the stroke patients were also distributed in the brainstem of lesioned hemisphere, and a few in bilateral frontal lobes, which may be degenerative lesions caused by Wallerian degeneration.

Neural changes contains anterograde, retrograde degeneration or refactoring, acute and chronic phases of stroke probably differ in the white matter changes. However, no matter what kind of alteration in brain generates specific structure with corresponding function. Therefore we did pattern recognition classification using the whole brain FA map and explored brain regions important for distinguishing patients with motor impairment from healthy controls.

Our study verified degenerative changes in white matter of stroke patients. The patients were infarcted mainly in the basal ganglia region, but the FA reduction of some remote areas has reached the point where they can be differentiated from the controls, so the changes have generality in some way.

Decreased WM connection in widely distributed brain areas of stroke patients

Many patients left with motor dysfunction after the occurrence of cerebral infarction. Usually, it is related to the injury of the corticospinal tract. The CST mainly originates from multiple motor and somatosensory cortices including premotor cortex, supplementary motor cortex (SMA), primary motor cortex, as well as primary and secondary somatosensory cortices. CST is crucial for proper execution of a

volitional movement [33,34]. Apart from CST and the motor areas of cortex, the proper execution of movements containing balance and coordination also requires extrapyramidal tract and other brain regions such as nucleus in basal ganglia and cerebellum [35]. Since the analysis is multivariate, all voxels in the white matter mask contribute to the decision function in the processing stage. We observed that the area where the left corticospinal tract passing is reddish, and there is a light green distribution in the corpus callosum and some other areas (Fig. 3). Combined with the NBS results, the affected brain tissue involved a wide range of brain regions (Fig. 5).

NBS analysis showed the structural subnetwork connection of the stroke group was weaker than that of the control group, which indicate that the nerve fibers involved in the subnetwork were affected. When the integrity and order of the brain structure were destroyed, it can be reflected in the white matter. Not only the brain regions directly related to the motor commands (e.g. precentral and SMA) were involved in the subnetwork, but also some regions that may participate in the regulation of motor control.

Next, we briefly discuss the brain regions contained in the subnetwork of NBS results.

The bilateral frontal lobe

Similar to the previous study, infarcts cause motor area focal thinning in remote cortex via degeneration of inter-hemispheric connection fiber of the corpus callosum [36,37], we found a change in the connection between the frontal hemispheres, and a small area in contralesional frontal cortex decreased in FA value. It has been reported that secondary degeneration occurred in the ipsilesional precentral gyrus after subcortical stroke involving the CST at the 6-month follow-up in stroke patients by calculating the mean kurtosis (MK) value of manually drawing ROI from Diffusion kurtosis imaging (DKI) imaging study [38]. Now we speculate the degeneration in remote parts of CST occurred in acute and subacute phases of stroke.

In addition to motor related brain areas, the affected brain areas in frontal lobe may generate mild or long-term cognitive changes in patients. Recently, a research reported the Reading the Mind in the Eyes Test (RMET) were associated with damage to white-matter tracts connecting frontal and temporo-parietal components of the RMET functional network [39]. Cognitive impairment still requires sensitive detection of subtle changes by complex experimental design or long-term observation [40].

Basal ganglia region

The patients were infarcted mainly in the basal ganglia region, the CST passing through posterior limb of internal capsule may receive regulation information from nucleus of basal ganglia or constitute loops with them. Due to the cortico-basal ganglia-thalamocortical ‘motor’ loop, any impact on the circuit constituent can lead to a shift in the balance between neural interactions in the direct and indirect pathways and subsequent variations in the brain functioning [41,42]. In the early stage of rehabilitation, stroke patients with hemiplegia often have synergistic movement, which is speculated to be related to this loop.

The occipital lobe

In our study, changes in white matter connections involving the occipital (cuneus and precuneus) are most likely related to visual effects. Voluntary actions modulate perception that follow the anatomical-functional bias of the motor system, in stroke patients with dysfunction of normal voluntary movement, they may develop corresponding abnormal sensory modulation that affect brain structure gradually [43]. A study observed reduced functional connectivity between motor and executive control and visuospatial networks in patients with motor deficits vs. healthy controls [44].They demonstrated functional connectivity exists between visual cortex and ipsilateral/ contralateral motor cortex and cerebellum. We conformed that this decline in functional connectivity is probably accompanied by a decrease in white matter structural connectivity.

Cerebellum

Cerebellum is often related to balance adjustment, patients with hemiplegia after stroke usually have problems in walk stability and coordination. The connections between the cerebrum and the cerebellum pass through the cerebral peduncle in brainstem, so we assume that the weakening of connections to the cerebellum is partially consistent with the decrease in FA in brainstem. Previous DTI studies also found a decrease in FA in midbrain after stroke by manually plotting ROI [38]. A recent study found the role of the cerebellum for residual motor output by facilitating cortical excitability in chronic stroke [45]. The changes of cortico-cerebellar structural connectivity was probably caused by brain injuries related to the neural fibers connecting to cerebellum, but the inability of normal movement may gradually lead to abnormal balance that reflected in the decreases of cortico-cerebellar connectivity.

Limitations and Expectations

Despite our significant findings, this research is not free of limitations. First, the sample size is small. Second, the range of MRI scan time from disease onset was wide and the phases of stroke rehabilitation may influence some white matter organization in an unexplored way, although we only discussed the stroke patients with motor impairment in a cross-sectional insight. Future work can be further explored by expanding the sample size and dynamically observing imaging changes from the acute phase to the recovery phase. And it should be emphasized on the classification and refinement of clinical behavior in stroke patients, with the changes of brain features that correspond to the functional outcome.

A study on 132 stroke patients using rest-fMRI has revealed that although structural damage from stroke is focal, remote dysfunction can occur in regions of the brain distant from the area of damage. These results link key organizational features of brain networks to brain behavior relationships in stroke [46].

By now, there is no large-scale post-stroke structural network analysis similar to the above functional analysis in quantity and method. In this study, only stroke patients with motor dysfunction were recruited for analysis using DTI data. By MVPA and NBS, we detected distribution of abnormal FA values and white matter connections in the whole brain of the stroke patients.

We need further investigate the changes of the brain structure or functional network in the natural process of different types of brain injuries. Then the diagnosis and prognosis can be concluded more precisely, the basis theory and guidance for the selection of treatment and research methods be provided more reasonably.

Conclusions

In summary, we found that there are multiple WM structural abnormalities in the affected brain areas of stroke patients with motor impairment. Our study may provide a basis for the further exploration of neural mechanism of the residual motor deficits in stroke patients.

Looking forward, in the future long-term prognosis research, we will further compare the neural changes of well-recovered patients to provide a basis of suggestions for the development of rehabilitation training strategies.

Abbreviations

DTI: Diffusion tensor imaging; MVPA: multivariate pattern analysis; NBS:network-based statistic; AAL: Automated Anatomical Labeling; FA:fractional anisotropy; MRI: Magnetic Resonance Imaging; WM: white matter; MD: mean diffusivity; RD: radial diffusivity; CST: corticospinal tract; ROI: region of interest ; MNI: Montreal Neurological Institute; FMA: Fugl-Meyer assessment; BRS: Brunnstrom stage; WD: Wallerian degeneration; DKI: Diffusion kurtosis imaging; RMET: Reading the Mind in the Eyes Test.

Declarations

Ethics approval and consent to participate

The study was approved by the local Ethics Committee of the Southeast University affiliated Zhongda Hospital. All participants gave written informed consent to participate according to the Declaration of Helsinki.

Consent for publication

Not applicable.

Availability of data and materials

The data in the current study are available on reasonable request from the corresponding author.

Competing interests

The authors declare that they have no competing interests

Funding

This work was funded by the National Natural Science Foundation of China (grant number:6590000127 , 81801680), Nanjing health science and technology development special fund project (grant number: YKK18218).

Authors' contributions

X.C. and Y.G. conceived and designed the research. X.C., Z.W, X.C. and Y.L. performed the experiments and analyzed the data. X.Y. and W.W. provided technical assistance. I.A., S.Y., X.G. and S.W. provided experimental assistance. X.C. and Y.G. wrote the manuscript.

Acknowledgements

We thank all the patients and volunteers for participating in this study.

References

1. Lim JS, Kang DW. Stroke Connectome and Its Implications for Cognitive and Behavioral Sequela of Stroke. J Stroke. 2015;17:256–67. https://doi.org/10.5853/jos.2015.17.3.256.
2. Cunningham DA, Machado A, Janini D, et al. Assessment of Inter-Hemispheric Imbalance Using Imaging and Noninvasive Brain Stimulation in Patients With Chronic Stroke. Arch Phys Med Rehabil. 2015;96:94–103. https://doi.org/10.1016/j.apmr.2014.07.419.
3. Visser MM, Nawaf Y, Campbell BCV, et al. White Matter Degeneration after Ischemic Stroke: A Longitudinal Diffusion Tensor Imaging Study. J Neuroimaging. 2018;29:111–8. https://doi.org/10.1111/jon.12556.
4. Byblow WD, Stinear CM, Barber PA, et al. Proportional recovery after stroke depends on corticomotor integrity. Ann Neurol. 2015;78:848–59. https://doi.org/10.1002/ana.24472.
5. Feng W, Wang J, Chhatbar PY, et al. Corticospinal tract lesion load - an imaging biomarker for stroke motor outcomes. Ann Neurol. 2015;78:860–70. https://doi.org/10.1002/ana.24510.
6. Meier EL, Johnson JP, Pan Y, et al. The utility of lesion classification in predicting language and treatment outcomes in chronic stroke-induced aphasia. Brain Imaging Behav. 2019;13:1510. https://doi.org/10.1007/s11682-019-00118-3.
7. Umarova RM, Beume L, Reisert M, et al. Distinct white matter alterations following severe stroke. Neurology. 2017;88:1546–55. https://doi.org/10.1212/WNL.0000000000003843.
8. Jang SH, Kim K, Kim SH, et al. The relation between motor function of stroke patients and diffusion tensor imaging findings for the corticospinal tract. Neurosci Lett. 2014;572:1–6. https://doi.org/10.1016/j.neulet.2014.04.044.
9. Lao Z, Shen D, Xue Z, et al. Morphological classification of brains via high-dimensional shape transformations and machine learning methods. Neuroimage. 2004;21:46–57. https://doi.org/10.1016/j.neuroimage.2003.09.027.
10. 10.1016/j.neuroimage.2008.11.007

Pereira F, Mitchell T, Botvinick M. Machine learning classifiers and fMRI: A tutorial overview. NeuroImage 2009;45:S199-S209. https://doi.org/10.1016/j.neuroimage.2008.11.007.

11. Li F, Huang X, Tang W, et al. Multivariate pattern analysis of DTI reveals differential white matter in individuals with obsessive-compulsive disorder. Hum Brain Mapp. 2014;35:2643–51. https://doi.org/10.1002/hbm.22357.
12. Janssen RJ, Mourão-Miranda J, Schnack HG. Making individual prognoses in psychiatry using neuroimaging and machine learning. Biol Psychiatr Cogn Neurosci Neuroimaging 2018;3:798–808. https://doi.org/10.1016/ j.bpsc.2018.04.004.
13. Zalesky A, Fornito A, Bullmore ET. Network-based statistic: Identifying differences in brain networks. NeuroImage. 2010;53:1197–207. https://doi.org/10.1016/j.neuroimage.2010.06.041.
14. Fortanier E, Grapperon A-M, Le Troter A, et al. Structural Connectivity Alterations in Amyotrophic Lateral Sclerosis: A Graph Theory Based Imaging Study. Front Neurosci. 2019;13:12. https://doi.org/10.3389/fnins.2019.01044.
15. Feng W, Wang J, Chhatbar PY, et al. Corticospinal Tract Lesion Load: An Imaging Biomarker for Stroke Motor Outcomes. Ann Neurol. 2015;78:860–70. https://doi.org/10.1002/ana.24510.
16. Naghdi S, Ansari NN, Mansouri K, et al. Neurophysiological and clinical study of Brunnstrom recovery stages in the upper limb following stroke. Brain Inj. 2010;24:1372–8. https://doi.org/10.3109/02699052.2010.506860.
17. Grefkes C, Nowak DA, Eickhoff SB, et al. Cortical connectivity after subcortical stroke assessed with functional magnetic resonance imaging. Ann Neurol. 2008;63:236–46. https://doi.org/10.1002/ana.21228.
18. Chen JL, Schlaug G. Resting state interhemispheric motor connectivity and white matter integrity correlate with motor impairment in chronic stroke. Front Neurol. 2013;4:178. https://doi.org/10.3389/fneur.2013.00178.
19. Zhang Y, Liu H, Wang L, et al. Relationship between functional connectivity and motor function assessment in stroke patients with 26 hemiplegia: a resting-state functional MRI study. Neuroradiology 2016;58:503–11. https://doi.org/10.1007/ s00234-016-1646-5.
20. Cui Z, Zhong S, Xu P, et al. PANDA: a pipeline toolbox for analyzing brain diffusion images. Front Hum Neurosci. 2013;7:42. https://doi.org/10.3389/fnhum.2013.00042.
21. Guo X, Liu R, Lu J, et al. Alterations in Brain Structural Connectivity After Unilateral Upper-Limb Amputation. IEEE Trans Neural Syst Rehabil Eng. 2019;27:2196–204. https://doi.org/10.1109/TNSRE.2019.2936615.
22. Mori S, Crain BJ, Chacko VP, et al. Three-Dimensional Tracking of Axonal Projections in the Brain by Magnetic Resonance Imaging. Ann Neurol 1999;45:265–269. https://doi.org/10.1002/1531-8249(199902)45:2<265::AID-ANA21>3.0.CO;2-3
23. Tzourio-Mazoyer N, Landeau B, Papathanassiou D,et al. Automated anatomical labeling of activations in spm using a macroscopic anatomical parcellation of the mni mri single-subject brain. Neuroimage. 2002;15:273–89. https://doi.org/10.1006/nimg.2001.0978.

24. Ni S, Yaou L, Kuncheng L, et al. Diffusion Tensor Tractography Reveals Disrupted Topological Efficiency in White Matter Structural Networks in Multiple Sclerosis. Cereb Cortex. 2011;21:2565–77. https://doi.org/10.1093/cercor/bhr039.
25. Schrouff J, Rosa MJ, Rondina JM, et al. PRoNTo: Pattern Recognition for Neuroimaging Toolbox. Neuroinformatics. 2013;11:319–37. https://doi.org/10.1007/s12021-013-9178-1.
26. Wang J, Wang X, Xia M, et al. GRETNA: a graph theoretical network analysis toolbox for imaging connectomics. Front Hum Neurosci. 2015;9:386. https://doi.org/10.3389/fnhum.2015.00386.
27. Xia M, Wang J, He Y. BrainNet Viewer: A Network Visualization Tool for Human Brain Connectomics. Plos One. 2013;8:e68910. https://doi.org/10.1371/journal.pone.0068910.
28. Liang YL, Cai X, Zhou H,et al. Voxel-based analysis and multivariate pattern analysis of diffusion tensor imaging study in anti-NMDA receptor encephalitis. Neuroradiology. 2020;62:231–9. https://doi.org/10.1007/s00234-019-02321-x.
29. Ecker C, Rocha-Rego V, Johnston P, et al. Investigating the predictive value of whole-brain structural MR scans in autism: A pattern classification approach. NeuroImage. 2010;49:44–56. https://doi.org/10.1016/j.neuroimage.2009.08.024.
30. Burke Quinlan E, Dodakian L, See J, et al. Neural function, injury, and stroke subtype predict treatment gains after stroke. Ann Neurol. 2015;77:132–45. https://doi.org/10.1002/ana.24309.
31. Virta A, Barnett A, Pierpaoli C. Visualizing and characterizing white matter fiber structure and architecture in the human pyramidal tract using diffusion tensor MRI. Magn Reson Imaging. 1999;17:1121–33. https://doi.org/10.1016/s0730-725x(99)00048-x.
32. Thomalla G, Glauche V, Koch MA, et al. Diffusion tensor imaging detects early Wallerian degeneration of the pyramidal tract after ischemic stroke. NeuroImage. 2004;22:1767–74. https://doi.org/10.1016/j.neuroimage.2004.03.041.
33. Lemon RN. Descending pathways in motor control. Annu Rev Neurosci. 2008;31:195–218. https://doi.org/10.1146/annurev.neuro.31.060407.125547.
34. Chenot Q, Tzourio-Mazoyer N, Rheault F, et al. A population-based atlas of the human pyramidal tract in 410 healthy participants. Brain Struct Funct. 2019;224:599–612. https://doi.org/10.1007/s00429-018-1798-7.
35. Moreno-López Y, Olivares-Moreno R, Cordero-Erausquin M, et al. Sensorimotor integration by corticospinal system. Front Neuroanat 2016;10. https://doi.org/10.3389/fnana.2016.00024.
36. Duering M, Righart R, Wollenweber FA, et al. Acute infarcts cause focal thinning in remote cortex via degeneration of connecting fiber tracts. Neurology. 2015;84:1685–92. https://doi.org/10.1212/WNL.0000000000001502.
37. Hayward KS, Neva JL, Mang CS, et al. Interhemispheric Pathways Are Important for Motor Outcome in Individuals with Chronic and Severe Upper Limb Impairment Post Stroke. Neural Plast. 2017;2017:1–12. https://doi.org/10.1155/2017/4281532.
38. Wei XE, Shang K, Zhou J, et al. Acute Subcortical Infarcts Cause Secondary Degeneration in the Remote Non-involved Cortex and Connecting Fiber Tracts. Front Neurol. 2019;10:9.

https://doi.org/10.3389/fneur.2019.00860.
39. Dominguez JFD, Nott Z, Horne K, et al. Structural and functional brain correlates of theory of mind impairment post-stroke. Cortex. 2019;121:427–42. https://doi.org/10.1016/j.cortex.2019.09.017.
40. Lim JSN, Kim MU, Jang MK, et al. Cortical Hubs and Subcortical Cholinergic Pathways as Neural Substrates of Poststroke Dementia. Stroke. 2014;45:1069–76. https://doi.org/10.1161/STROKEAHA.113.004156.
41. Alexander GE, Crutcher MD, DeLong MR. Basal ganglia-thalamocortical circuits: parallel substrates for motor, oculomotor, "prefrontal" and "limbic" functions. Prog Brain Res. 1990;85:119. https://doi.org/10.1016/S0079-6123(08)62678-3.
42. Silkis I. The cortico-basal ganglia-thalamocortical circuit with synaptic plasticity. II. Mechanism of synergistic modulation of thalamic activity via the direct and indirect pathways through the basal ganglia. Biosystems. 2001;59:7–14. https://doi.org/10.1016/S0303-2647(00)00135-0.
43. Buaron B, Reznik D, Gilron R, et al. Voluntary actions modulate perception and neural representation of action-consequences in a hand-dependent manner. 2020 [Preprint] https://www.researchgate.net/publication/338586442 https://doi.org/10.1101/2020.01.12.90305444.
44. Almeida SRM, Vicentini J, Bonilha L, et al. Brain connectivity and functional recovery in patients with ischemic stroke. J Neuroimaging. 2017;27:65–70. https://doi.org/10.1111/jon.12362.
45. Guder S, Frey BM, Backhaus W, et al. The Influence of Cortico-Cerebellar Structural Connectivity on Cortical Excitability in Chronic Stroke. Cereb Cortex. 2020;30:1330–44. https://doi.org/10.1093/cercor/bhz169.
46. Siegel JS, Ramsey LE, Snyder AZ, et al. Disruptions of network connectivity predict impairment in multiple behavioral domains after stroke. Proc Natl Acad Sci U S A. 2016;113:E4367–76. https://doi.org/10.1073/pnas.1521083113.

Figures

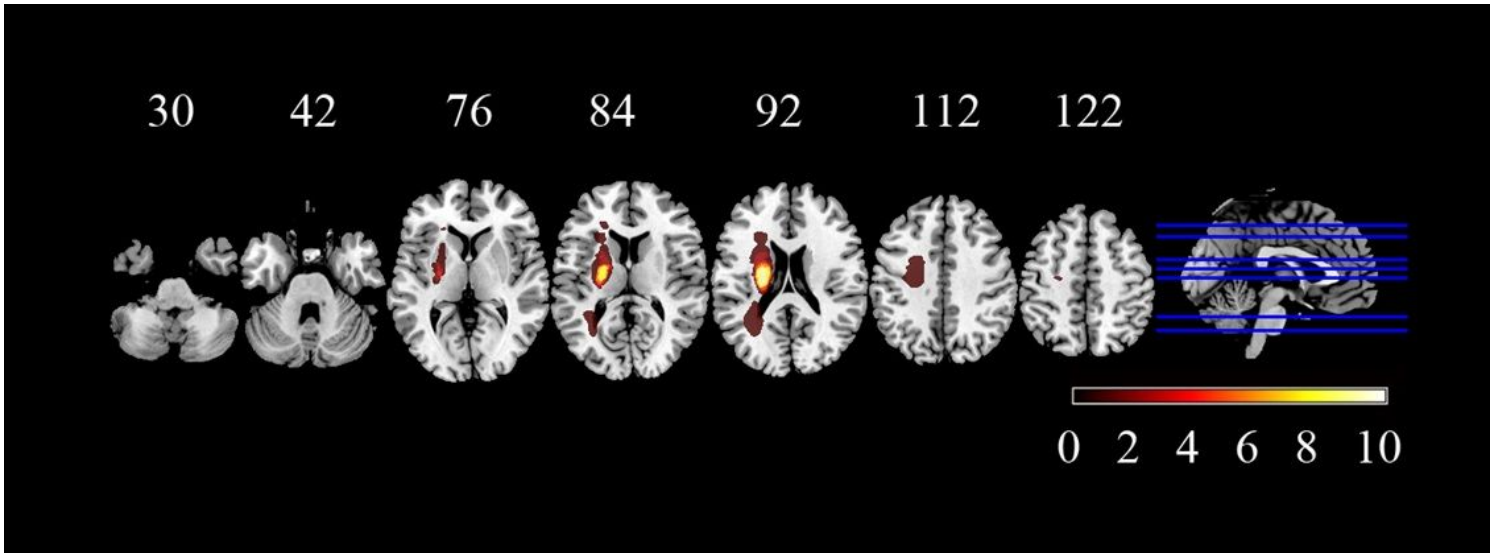

Figure 1

Lesion incidence map of patients with stroke. Stroke lesions were projected to the left hemisphere for each patient and overlaid onto a T1 template in MNI standard space. Colorbar indicates the number of patients with stroke lesions in the corresponding voxel. Z values mark the MNI coordinates of the transverse section.

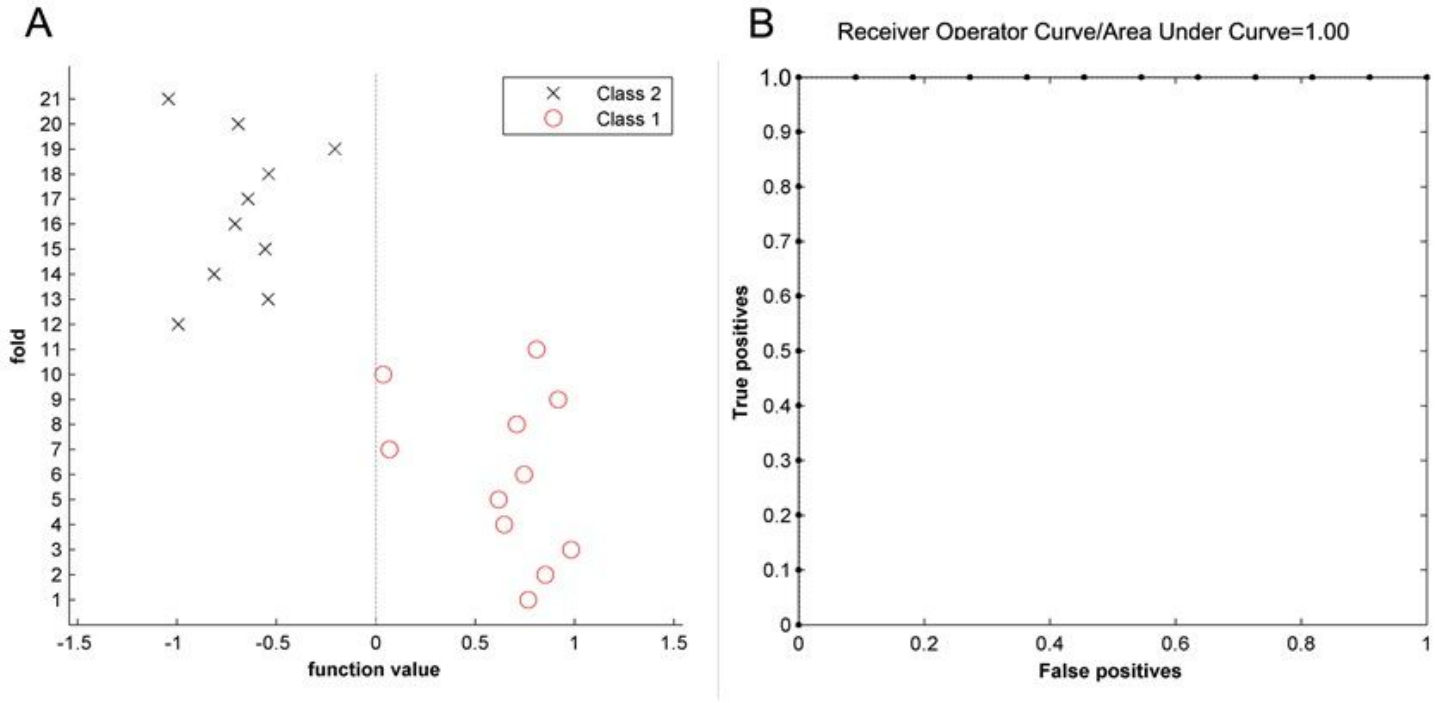

Figure 2

The result of the MVPA classification. Classification plot (A) and Receiver Operating Characteristic (ROC) curve (B) for the comparison between stroke patients and controls using FA maps from DTI data, which yielded an accuracy of 100% (100% sensitivity, 100% specificity), statistically significant at $P \leq 0.001$.

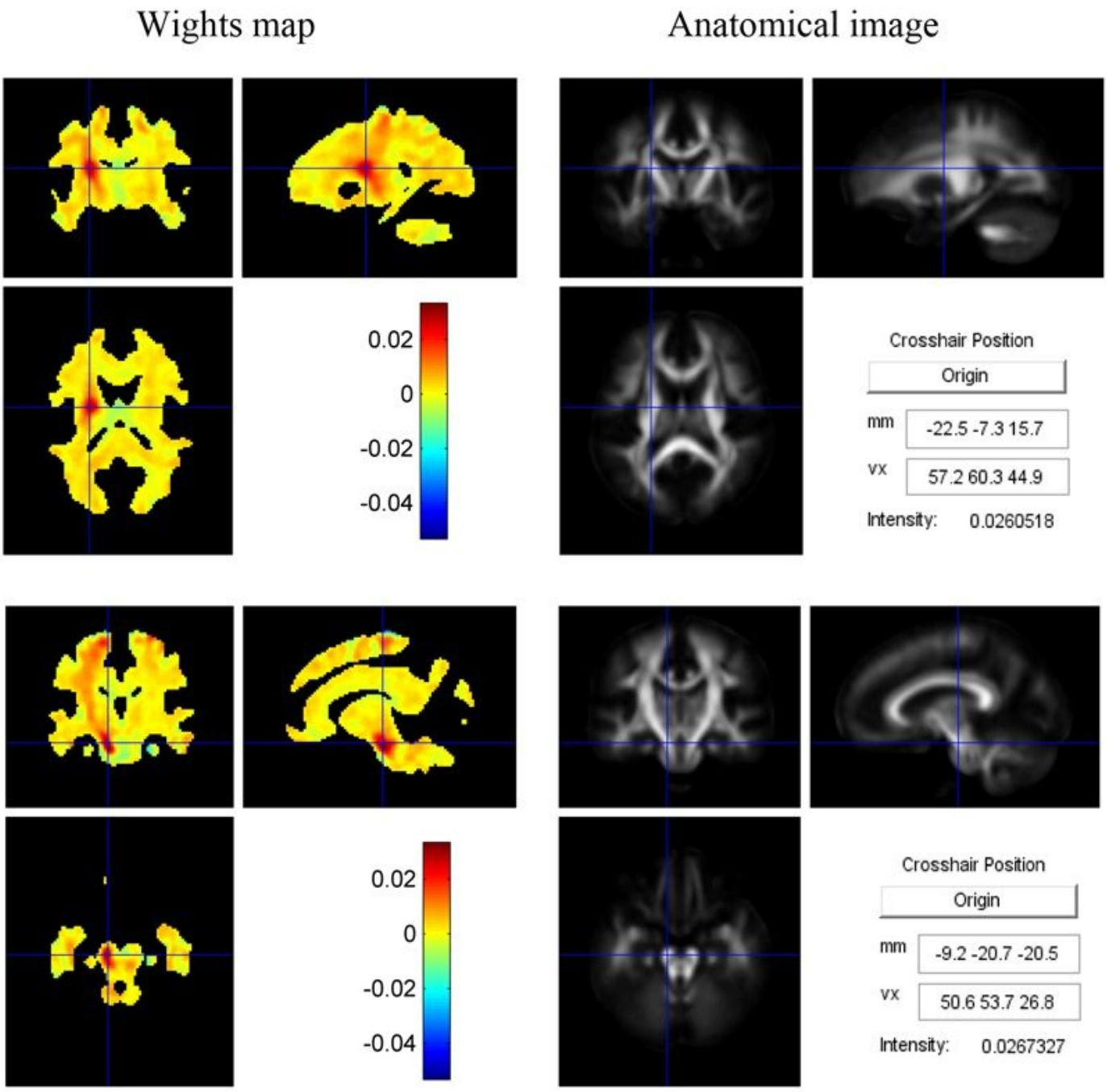

Figure 3

Whole-brain voxel weight map. It shows the white matter regions contributing to discrimination between groups based on FA values. The colour bar indicates the weight vector value of the voxel, which is also indicated in the intensity field of the Anatomical image (white fiber atlas 'JHU-ICBM-FA-2mm') panel.

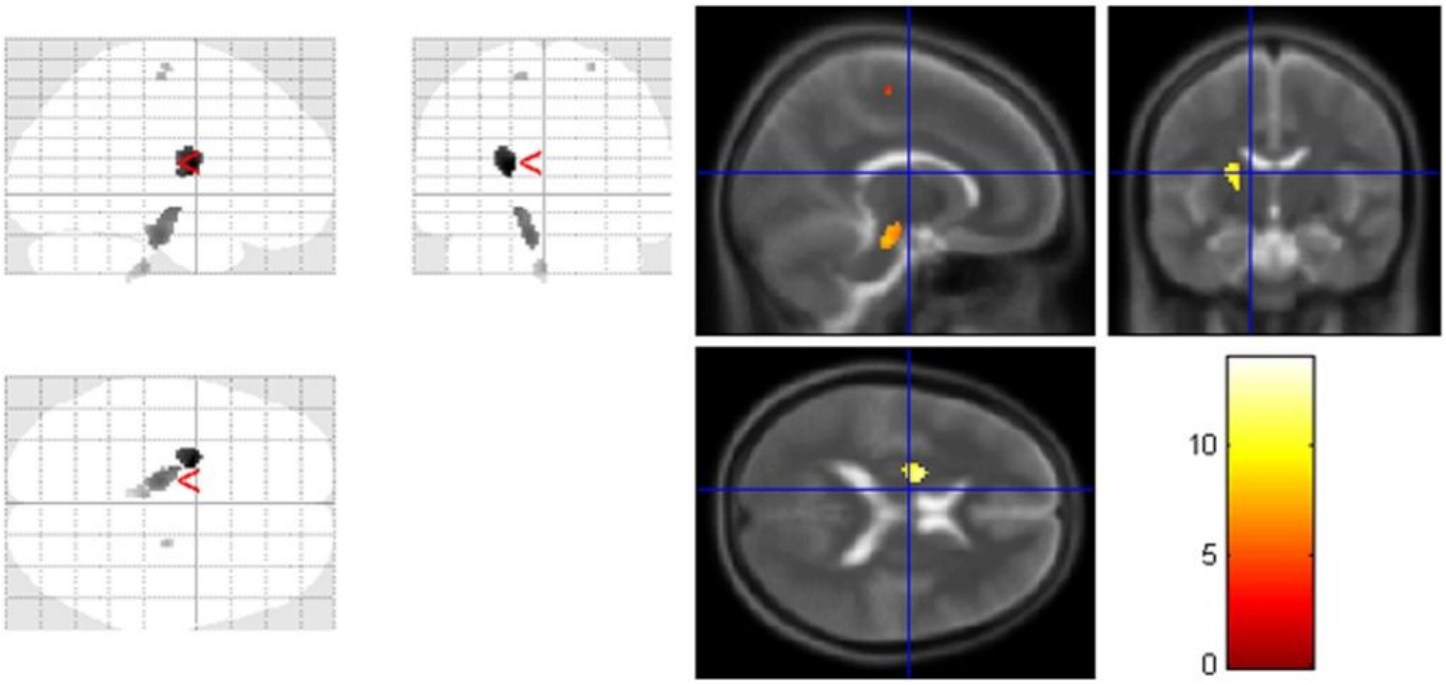

Figure 4

FA decreased brain area in patients compared to controls. Also, these regions were identified by setting the threshold to ≥ 30% of the maximum weight vector scores on the basis of whole-brain voxel weight map. The colour bar indicates the T value in two-sample t tests.

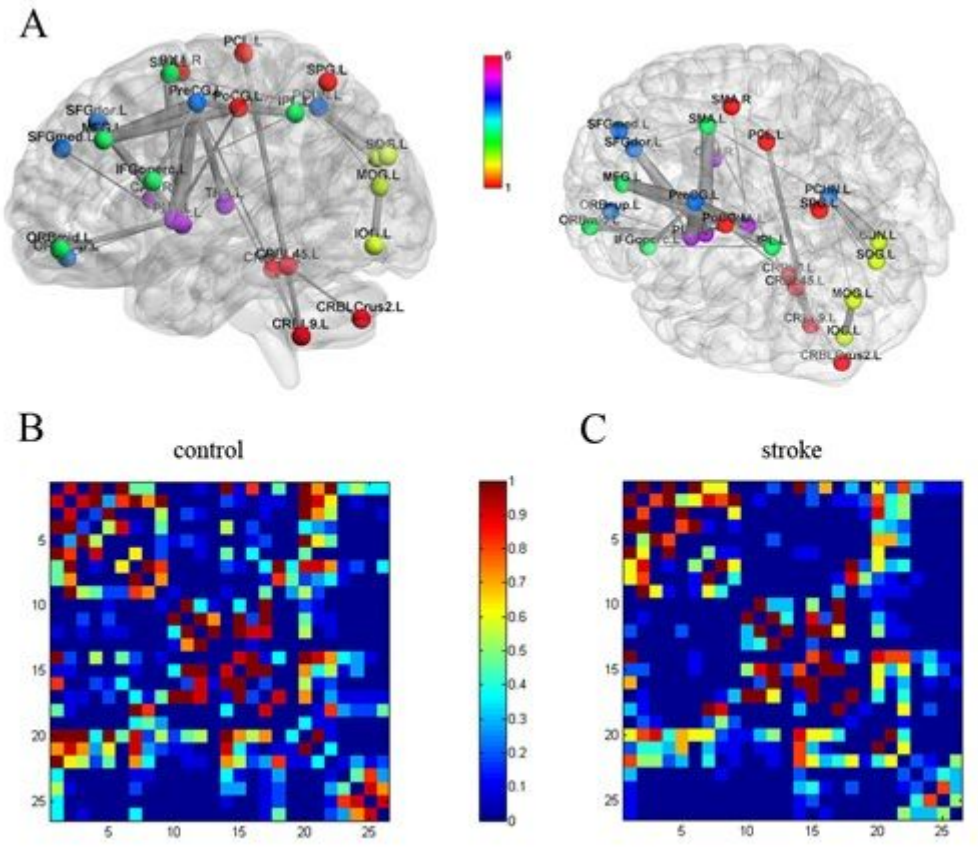

Figure 5

Subnetwork identified by the network-based statistics (NBS) analysis. (A) Subnetwork demonstrated reduced connectivity in stroke patients compared to controls. The colorbar indicates connection probability in groups. The group averaged FA-weighted structural connectivity network for control group(B) and stroke group(C) (circles represent regions that were affected by the white matter disruption, the colors indicate different modules; thickness of edges represents how significantly 2 groups are different).

Supplementary Files

This is a list of supplementary files associated with this preprint. Click to download.

- movie.avi